Since January 2020 Elsevier has created a COVID-19 resource centre with free information in English and Mandarin on the novel coronavirus COVID-19. The COVID-19 resource centre is hosted on Elsevier Connect, the company's public news and information website.

Toxicology and Applied Pharmacology 356 (2018) 90–97

Contents lists available at ScienceDirect

Toxicology and Applied Pharmacology

journal homepage: www.elsevier.com/locate/taap

The cardenolide ouabain suppresses coronaviral replication via augmenting a Na^+/K^+-ATPase-dependent PI3K_PDK1 axis signaling

Cheng-Wei Yang, Hsin-Yu Chang, Yue-Zhi Lee, Hsing-Yu Hsu, Shiow-Ju Lee*

Institute of Biotechnology and Pharmaceutical Research, National Health Research Institutes, Miaoli 35053, Taiwan, ROC

ARTICLE INFO

Keywords:
Cardenolide
Coronavirus
Na^+/K^+-ATPase
Ouabain
PI3K
PDK1

ABSTRACT

Cardenolides are plant-derived toxic substances. Their cytotoxicity and the underlying mechanistic signaling axes have been extensively documented, but only a few anti-viral activities of cardenolides and the associated signaling pathways have been reported. Previously, we reported that a variety of cardenolides impart anti-transmissible gastroenteritis coronavirus (TGEV) activity in swine testicular (ST) cells, through targeting of the cell membrane sodium/potassium pump, Na^+/K^+-ATPase. Herein, we further explore the potential signaling cascades associated with this anti-TGEV activity in ST cells. Ouabain, a representative cardenolide, was found to potently diminish TGEV titers and inhibit the TGEV-induced production of IL-6 in a dose dependent manner, with 50% inhibitory concentrations of 37 nM and 23 nM respectively. By pharmacological inhibition and gene silencing, we demonstrated that PI3K_PDK1_RSK2 signaling was induced in TGEV-infected ST cells, and ouabain imparted a degree of anti-TGEV activity via further augmentation of this existing PI3K_PDK1 axis signaling, in a manner dependent upon its association with the Na^+/K^+-ATPase. Finally, inhibition of PI3K by LY294002 or PDK1 by BX795 antagonized the anti-viral activity of ouabain and restored the TGEV virus titer and yields. This finding is the first report of a PI3K_PDK1 signaling axis further induced by ouabain and implicated in the suppression of TGEV activity and replication; greatly illuminates the underlying mechanism of cardenolide toxicity; and is expected to result in one or more anti-viral applications for the cardenolides in the future.

1. Introduction

Cardenolides are plant-derived toxic substances, used in small doses to treat hypotension and some arrhythmias; and recently discovered to exert anti-cancer and antiviral activity by targeting and binding to their membrane receptor, the sodium/potassium pump Na^+/K^+-ATPase (Agrawal et al., 2012; Diederich et al., 2017). This direct binding of cardenolides to Na^+/K^+-ATPase (located in the cell membrane) induces endocytosis, which reduces the amount of Na^+/K^+-ATPase at the cellular surface, perturbing the homeostasis of cell solutes, and hence elevating intracellular calcium levels (Diederich et al., 2017; Newman et al., 2008; Prassas and Diamandis, 2008). Exploration of novel anti-viral associated signaling axes of the cardenolides is expected to illuminate the underlying mechanisms of their toxicity.

Each isoform of Na^+/K^+-ATPase consists of three subunits: one alpha, one beta, and one gamma; of which there are four, three and one kind, respectively (Baker Bechmann et al., 2016; Diederich et al., 2017; Katz et al., 2015). While the alpha subunit of Na^+/K^+-ATPase is the most well-known cellular target of cardiac glycosides, their selectivity for the various isoforms of Na^+/K^+-ATPase varies due to the structural diversity of the alpha and beta subunits (Habeck et al., 2016; Katz et al., 2015).

The use of cardenolides to combat human cancers and reduce viral production has been previously explored (Diederich et al., 2017; Nagai et al., 1972; Platz et al., 2011; Su et al., 2008; Tomita and Kuwata, 1978). The binding of cardenolides to Na^+/K^+-ATPase not only inhibits the activity of the solute pump, but also results in the recruitment of Na^+/K^+-ATPase associated signalsomes in cancer cells, initiating the associated signaling pathways, and hence the anti-cardiovascular dysfunction and anti-cancer biological activities (Diederich et al., 2017; Newman et al., 2008; Prassas and Diamandis, 2008). These signalings are involved in Src-mediated cytostatic effects, cell death pathways (including non-apoptotic cell death, apoptosis, autophagy, or mitophagy), and nuclear events (including transcriptional activity, epigenetic effects) etc. (Diederich et al., 2017). However, only a few reports have investigated the antiviral mechanisms of cardenolides (Burkard et al., 2015; Yang et al., 2017a).

Transmissible gastroenteritis coronavirus (TGEV) infects pigs and causes transmissible gastroenteritis with high mortality (Weiss and Navas-Martin, 2005). TGEV spike (S) protein binds to porcine cell

* Corresponding author.
E-mail address: slee@nhri.org.tw (S.-J. Lee).

https://doi.org/10.1016/j.taap.2018.07.028
Received 7 May 2018; Received in revised form 10 July 2018; Accepted 23 July 2018
Available online 25 July 2018
0041-008X/

Table 1
Sequences of primers for RT-PCR.

Gene		Sequences
N protein	Forward	5′-CCAAGGATGGTGCCATGAAC-3′
	Reverse	5′-GGACTGTTGCCTGCCTCTAGA-3′
$3CL^{pro}$	Forward	5′-CACCAACTACAATGGCCACACA-3′
	Reverse	5′-TAGCCCTGGTAGGTGACTCTGTT-3′

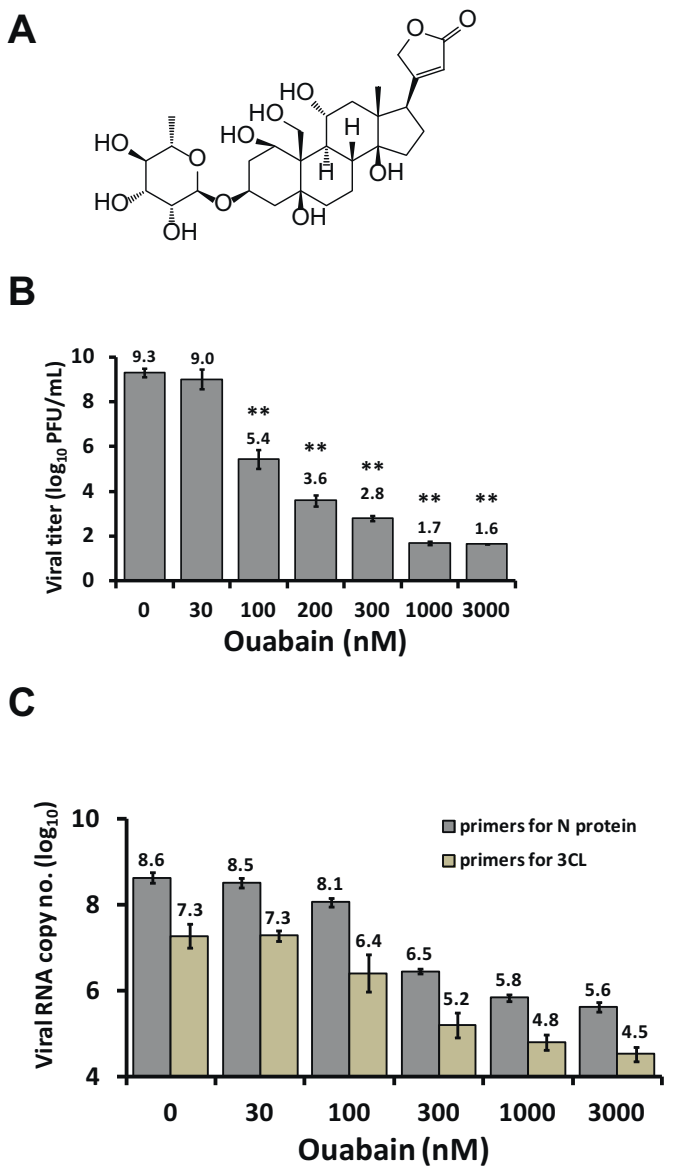

Fig. 1. Ouabain potently inhibits TGEV replication. A. Chemical structure of ouabain. B. Ouabain reduced TGEV yields in a dose-dependent manner in an end point assay for viral titer determination. C. Ouabain potently reduced TGEV viral copy number in ST cells by TGEV infection in a dose-dependent manner, as measured by RT-qPCR. ST cells were pretreated with ouabain for 1 h and then infected with TGEV at a multiplicity of infection (MOI) of 0.01 at 22 h.p.i. for determining virus titers (B) and at an MOI of 7 at 6 h.p.i. for determining viral copy numbers (C). See Materials and Methods for determination of the viral copy numbers and Table 1 for the primer sequences used for RT-qPCR. Results shown are averages ± SD from three independent experiments (B & C) each conducted in triplicate (C).

receptor aminopeptidase N, to aide in the entry of TGEV into cells. Swine testicular (ST) cells have been used as a host cell line for TGEV in many studies since the 1990s because ST cells express aminopeptidase

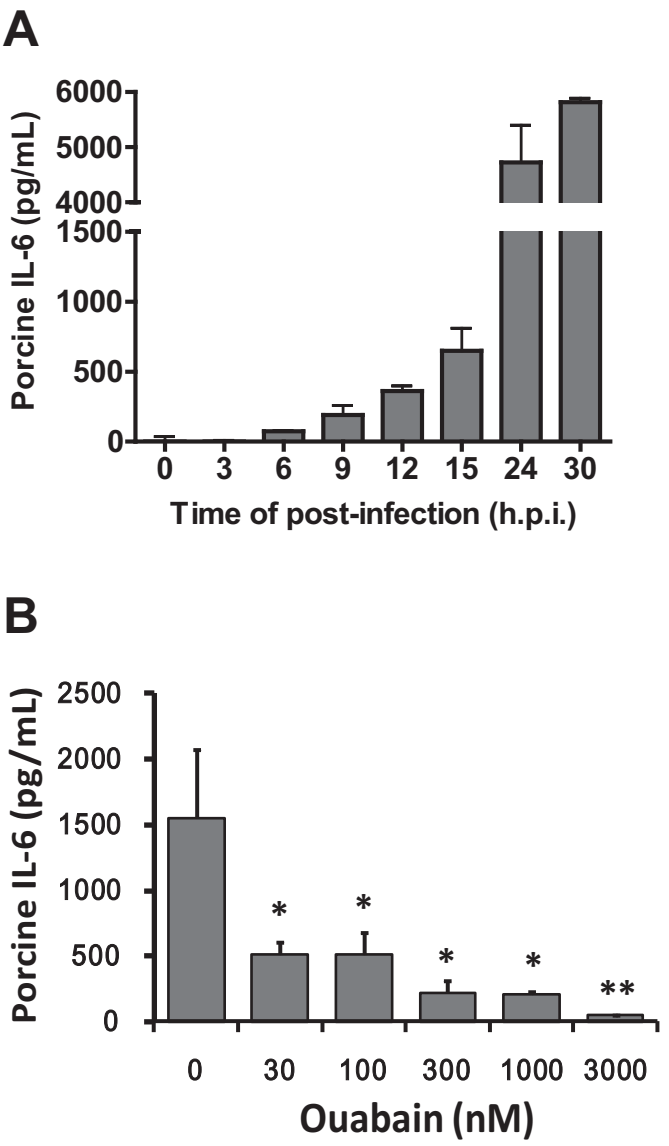

Fig. 2. Ouabain potently inhibited the IL-6 induction in ST cells by TGEV infection. A. ST cells were induced to produce a large quantity of IL-6 upon TGEV infection at MOI of 0.01 over a period of 30 h.p.i. The resultant culture supernatant of TGEV infected ST cells at each indicated time point was subjected to quantification of IL-6. B. IL-6 production in TGEV infected ST cells was significantly diminished by ouabain in a dose dependent manner. Ouabain was pretreated for 1 h prior to ST cells infected with TGEV at a MOI of 0.01. The resultant culture supernatants of ouabain treated cells at the 22 h.p.i. were subjected to quantification of IL-6. Results shown are averages ± SD from three independent experiments.

N and are highly susceptible to TGEV (Delmas et al., 1992; Oh et al., 2003; Weingartl and Derbyshire, 1995; Weiss and Navas-Martin, 2005). Previously, we reported that a variety of cardenolides (including ouabain) exert potent anti-TGEV activities (Yang et al., 2017a). While knocking down the expression of Na^+/K^+-ATPase decreases TGEV infectivity in ST cells (Yang et al., 2017a), the exact associated effective pathways remain to be investigated.

Herein, we disclosed the results of our studies into the underlying anti-TGEV mechanisms of ouabain. We found that ouabain enhanced an existing Na^+/K^+-ATPase-dependent PI3K_PDK1 signaling axis which was initially activated by TGEV infection in ST cells, and that this augmented Na^+/K^+-ATPase-dependent PI3K_PDK1 signaling axis activation by ouabain, contributing to anti-TGEV activity and replication.

Table 2
Screening of cellular signaling pharmacological inhibitors to identify those able to reverse the anti-TGEV effect of ouabain. Shown are residual activities by treatment of each pharmacological inhibitor compared to DMSO vehicle treatment which TGEV activity was used as 100%. IFA described in Methods for detection of N and S protein expression was applied to measure TGEV activity.

		Ouabain (μM)			
Inhibitor	μM	0.3	0.2	0.1	0
None		** 4% ± 2%	** 16% ± 3%	80% ± 6%	100% ± 0%
LY294002	50	** 21% ± 6%	** 40% ± 3%	83% ± 6%	89% ± 7%
	25	3% ± 2%	20% ± 3%	86% ± 12%	90% ± 8%
SU6656	50	6% ± 0%	13% ± 1%	46% ± 6%	95% ± 10%
	10	3% ± 1%	6% ± 0%	43% ± 7%	88% ± 1%
KX2-391	50	2% ± 1%	2% ± 0%	25% ± 4%	72% ± 5%
	20	4% ± 1%	3% ± 0%	43% ± 7%	74% ± 6%
PP2	50	1% ± 1%	15% ± 1%	52% ± 12%	89% ± 6%
	20	4% ± 2%	9% ± 1%	62% ± 18%	113% ± 11%
Rottlerin	2	3% ± 4%	5% ± 0%	75% ± 19%	78% ± 12%
GF109203X	1	2% ± 2%	13% ± 3%	52% ± 6%	105% ± 11%
FTA	10	5% ± 3%	11% ± 3%	96% ± 26%	106% ± 12%
Rac1	100	2% ± 1%	0% ± 0%	16% ± 6%	54% ± 3%
Wortmannin	1	5% ± 3%	10% ± 2%	90% ± 23%	102% ± 19%
Triciribine	20	3% ± 1%	8% ± 1%	78% ± 17%	90% ± 17%

** , <0.01, compare to ouabain only treatment

Results shown are averages ± SD from three independent experiments, each conducted in duplicate.
*P < .01, compare to only ouabain treatment.
**, < 0.01, compare to ouabain only treatment.

This discovery of a novel signaling axis, initiated upon the binding of ouabain to Na^+/K^+-ATPase, greatly illuminates the underlying mechanism of cardenolide toxicity, and is expected to result in one or more anti-viral applications for the cardenolides in the future.

2. Materials and methods

2.1. Cell lines, viruses, immunofluorescent assay (IFA) and multiplicity of infection (MOI) for infection

ST cells were purchased from ATCC (ATCC®CRL-1746TM) and cultured in minimum essential medium (MEM; Gibco, Grand Island, NY, USA), supplemented with 10% fetal bovine serum (FBS) (Biological Industries, Beit Haemek, Israel) and 1% penicillin–streptomycin (Biological Industries, Beit Haemek, Israel) in a humidified incubator of 5% CO_2 atmosphere at 37 °C. The Taiwan field isolated virulent strain of TGEV was propagated in ST cells cultured with MEM and 2% FBS. IFA and studies on the mechanistic signaling effectors regarding ouabain and the other pharmacological inhibitors in TGEV infected ST cells were performed as described (Yang et al., 2017a; Yang et al., 2017b). Briefly, the ST cells in 96-well plates, with or without pretreatment of test compounds, were infected with TGEV at an MOI of 7. After 6 h of TGEV infection, ST cells were fixed and subjected to an indirect IFA with antibodies against the S and nucleocapsid (N) proteins of TGEV. The cells were treated with eight different concentrations of test compounds. The resultant cells were incubated with fluorescein isothiocyanate-conjugated anti-mouse immunoglobulin (Cappel, ICN Pharmaceuticals Inc.) and the fluorescence intensities were measured to determine the 50% inhibitory concentrations (IC_{50}) for inhibiting S and N protein expression. The results of these assays were used to obtain the dose-response curves from which IC_{50}s were determined.

The test compounds were pretreated for 1 h and ST cells were infected with TGEV at (i) an MOI of 7 for IFA, analyses of signaling effectors and viral copy numbers at 6 h.p.i.; and (ii) an MOI of 0.01 for determining virus titers and IL-6 production at 22 h.p.i or indicated time points.

2.2. Chemicals and western blot analysis

Western blots were performed as described (Yang et al., 2007) with the following antibodies: p-Akt (S473), p-Akt (T308), Akt, p-p70S6K (T389), p70S6K, RSK1, p-RSK2 (S227), RSK2, p-PDK1 (S241), PDK1, PI3K p110α, and GAPDH (Cell Signaling Technology Inc., MA, USA); Na^+/K^+-ATPase α1 (Abcam Inc. Cambridge, UK); and an antibody against TGEV N protein, as described (Yang et al., 2007). Ouabain (O3125, ≧95%, HPLC) was purchased from Sigma-Aldrich (St. Louis, MO, USA). p-RSK1 (T359/S363) antibody, BX795, rottlerin, GF109203X, rapamycin, and triciribine were purchased from Merck Millipore Calbiochem (Billerica, MA). LY294002, PP2, KX2-391 and SU6656 were from Selleckchem (Houston, TX, USA). Farnesyl thiosalicylic acid (FTA, a Rac1 inhibitor) was purchased from Santa Cruz Biotechnology (Santa Cruz, CA). Wortmannin was purchased from Life Technologies (San Diego, CA, USA).

2.3. Viral RNA isolation and relative quantification by RT-qPCR

These experiments were performed as described (Yang et al., 2017b). Mock or TGEV infected (MOI of 7) ST cells were processed and the resultant cell lysates were prepared at 6 h.p.i., with or without compound treatment. Subsequently, total RNA was extracted with TRIzol reagent (Invitrogen) prior to RT-qPCR analyses. The primer pairs used for RT-qPCR are listed in Table 1. Viral copy numbers were determined as described (Yang et al., 2017b). Known amounts (numbers) of the plasmids pGEX6p-1-PEN (Yang et al., 2017b) and pGEX6p-TGEV-$3CL^{pro}$ (Yang et al., 2007) were used to establish standard curves for determination of TGEV viral copy numbers.

2.4. IL-6 cytokine measurement

The amount of porcine IL-6 cytokine was measured as described (Yang et al., 2017b). Briefly, the supernatant of TGEV infected ST cells at an MOI of 0.01 was harvested at the indicated periods and the amount of secreted IL-6 was determined using an enzyme-linked immunosorbent assay kit for porcine IL-6 (R&D Systems, Inc.). Appropriate dilutions were performed prior to determination of the amounts of IL-6 when the harvested supernatants contained concentrations of IL-6 too high to be accurately assayed using the enzyme-linked immunosorbent assay kit.

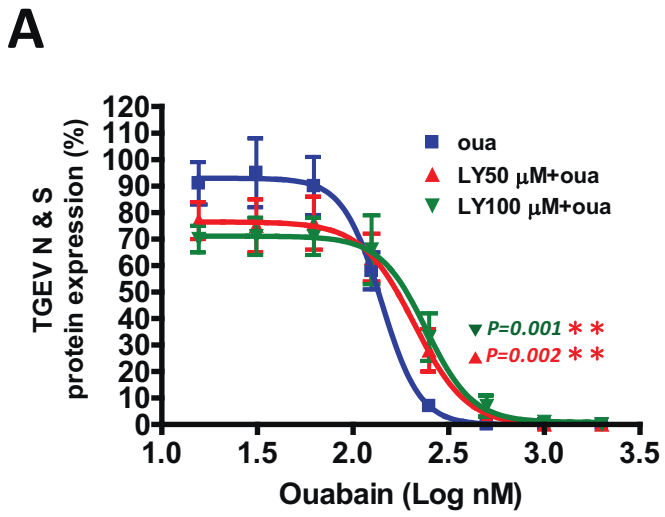

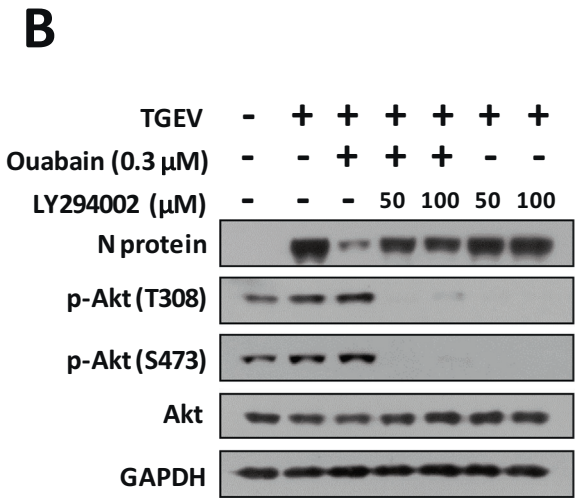

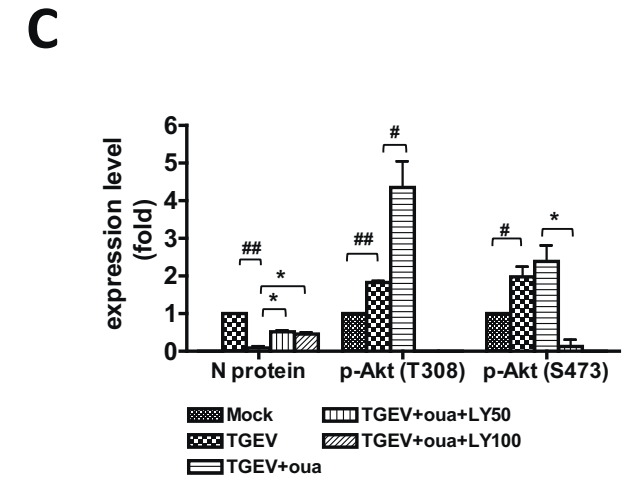

Fig. 3. PI3K inhibition antagonized the anti-TGEV activity of ouabain. A. PI3K inhibition by LY294002 attenuated the potency of the anti-TGEV activity of ouabain in an IFA assay by increasing the IC_{50} value and shifting the dose-dependent inhibition curve to right. B. PI3K inhibition by LY294002 rescued the TGEV N protein level, which was significantly inhibited by ouabain, as determined by western analysis. C. Quantification and statistical significance analysis of B. ST cells were pretreated with the indicated test compounds for 30 min, then treated with ouabain for 1 h prior to TGEV infection at an MOI of 7 for observation or fluorescent intensity measurements for IFA (A) or for western analysis with the indicated antibodies (B) at 6 h.p.i. ST cells were fixed and subjected to an indirect IFA with antibodies against the S and N proteins of TGEV. The obtained S and N protein expressions by IFA or western analysis were used as an indication of TGEV activity. * and #, $P < .05$; ** and ##, $P < .01$. #/##: was compared to TGEV infection control; */**: was compared to TGEV infection with ouabain treatment; N protein and p-Akt were normalized with GAPDH. Results shown are represented results (B) or averages ± SD from three independent experiments (A and C).

2.5. Gene silence

ST cells harbored ATP1A1 shRNA (clone ID: TRCN0000444902), PIK3CA shRNA#1 (clone ID:TRCN0000196582), PIK3CA shRNA#2: (clone ID: TRCN0000196795), PDPK1 shRNA#1 (clone ID: TRCN0000221540), PDPK1 shRNA #2: (clone ID:TRCN0000196933) or negative control-shRNAs (shLacZ, clone ID: TRCN0000231722 for ATP1A1; and shLacZ, clone ID: TRCN0000072224 for PIK3CA and PDPK1) (Academia Sinica, Taiwan) respectively for specific gene silencing were prepared as described previously (Yang et al., 2017a). After validation of Na^+/K^+-ATPase α1, PI3Kα or PDK1 knockdown expression, the selected cells were used for the followed experiments.

2.6. End point dilution assay for determining virus titers

Virus titers were determined by an end point dilution assay, as described (Yang et al., 2017a). Briefly, the supernatant obtained from the culture of TGEV infected ST cells (MOI of 0.01) at the 22 h.p.i. with the indicated treatment was subjected to viral titer determination via the end point dilution assay. The TCID50 (Tissue Culture Infective Dose 50%) was determined by the Reed-Muench method. TCID50 was then used to measure the infectious TGEV virus titer, as approximately 1 TCID = 0.69 PFU (plaque-forming unit).

2.7. Statistical analysis

The statistical significance between the two groups was evaluated by the two-tailed unpaired Student's *t*-test; * (or #) and ** (or ##) were used to denote the statistical significance for $p < .05$, and $p < .01$ respectively.

3. Results

3.1. Ouabain eliminated TGEV titers, inhibited viral replication, and diminished TGEV induced IL-6 production

Cardenolides have been previously found to potently inhibit TGEV activity in ST cells without significant cytotoxicity (concentration for 50% cytotoxicity against ST cells > 10 μM) (Yang et al., 2017a). We selected ouabain (Fig. 1A) to study the mechanism by which this inhibition occurs. After infection in ST cells, TGEV exhibited a log phase increase in viral yields and reached a plateau from 15 to 22 h.p.i. with

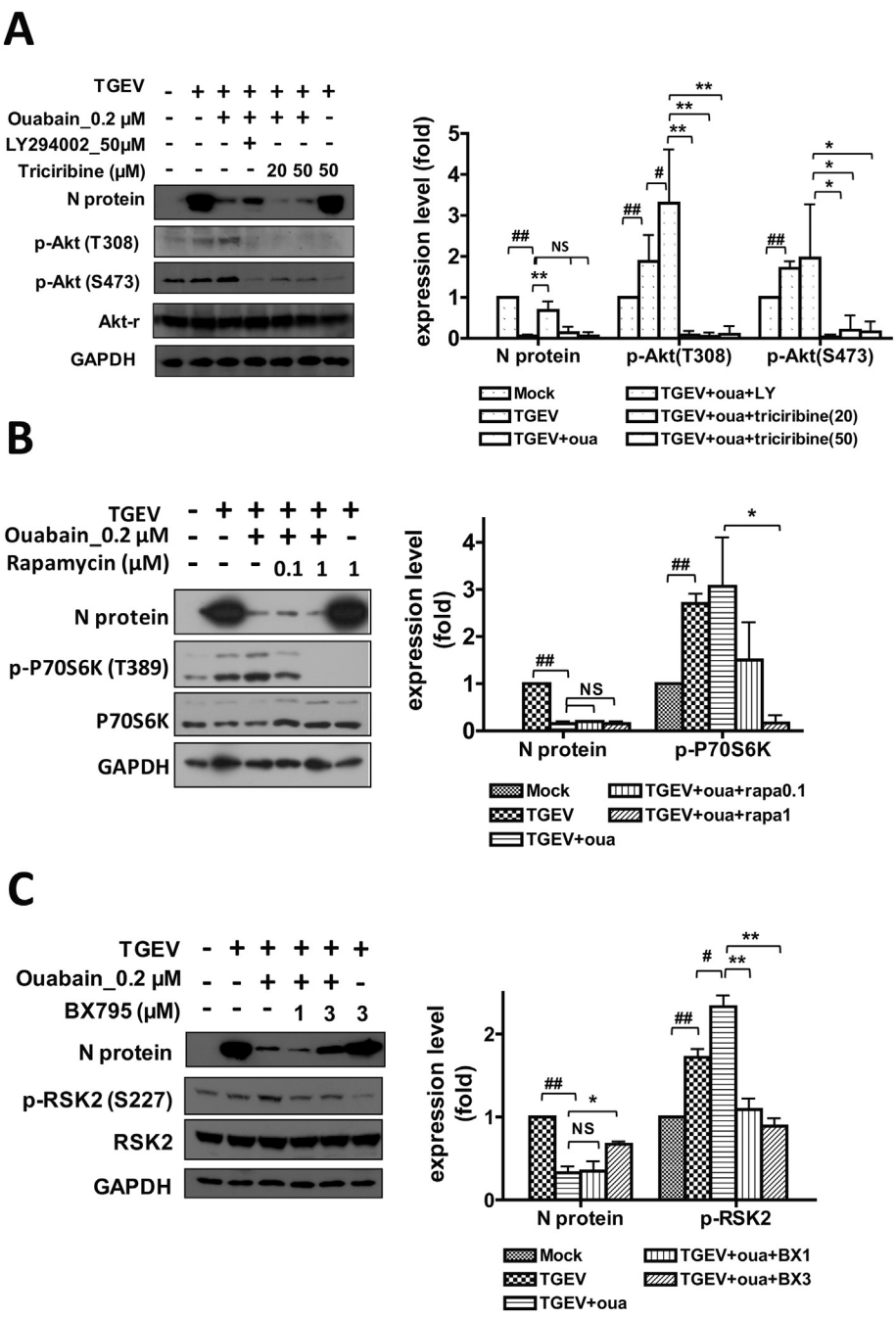

Fig. 4. Ouabain activates PI3K_PDK1 axis signaling that leads to an inhibition of TGEV activity. A. Ouabain anti-TGEV activity was not mediated by PI3K_Akt axis signaling. B. Ouabain anti-TGEV activity was not mediated by PI3K_mTOR axis signaling. C. Ouabain anti-TGEV activity was mediated by PI3K_PDK1axis signaling. ST cells were pretreated with the indicated test compounds for 30 min, then treated with ouabain for 1 h prior to TGEV infection at an MOI of 7 for 6 h, and the resultant cells were harvested for western analysis with the indicated antibodies. NS: no significance; * and #, $P < .05$; ** and ##, $P < .01$. #/##: was compared to TGEV infected control; */**: was compared to TGEV infection with ouabain treatment; N protein, p-Akt, and p-P70S6K, were normalized with GAPDH. p-RSK2 was normalized with regular RSK2. Results shown are represented results or averages ± SD from three independent experiments.

titers of ~10^9 p.f.u. /ml (Yang et al., 2017b). As expected, in TGEV infected ST cells with an MOI of 0.01 at 22 h.p.i., ouabain diminished both the viral titers and viral yields, even at low doses, in a dose-dependent manner with a 50% inhibitory concentration (IC_{50}) of 37 ± 15 nM. Ultimately, ouabain treatments at concentrations of 1000–3000 nM resulted in reductions of viral titer by ~7–8 orders of magnitude (Fig. 1B). Similarly, ouabain treatments resulted in the reduction of the number of viral RNA copies by ~3 orders of magnitude in TGEV infected ST cells, with an MOI of 7 at 6 h.p.i. (Fig. 1C). Moreover, TGEV infection (0.01 MOI) induced a sustained production of IL-6 over a 30 h period in ST cells (Fig. 2A); and this induction was profoundly diminished by ouabain in a dose dependent manner with an IC_{50} of 23 ± 2 nM (Fig. 2B).

3.2. Ouabain enhanced PI3K activation in TGEV infected ST cells contributed to anti-TGEV activity

To identify the signaling pathways involved in the anti-TGEV activity of ouabain, we comprehensively examined ouabain-related cellular events for anti-TGEV activity by screening a variety of pharmacological inhibitors for several signaling pathways (Table 2). LY294002, a PI3K inhibitor, significantly reversed the anti-TGEV activity of ouabain as determined by IFA (Table 2 & Fig. 3A) for viral S and N antigen expression. The anti-TGEV IC_{50} value of ouabain (IC_{50} = 143 ± 13 nM) increased in the presence of 50 μM or 100 μM LY294002 (IC_{50} = 171 ± 23 nM and IC_{50} = 182 ± 30 nM respectively), and the inhibition curve exhibited a significant right-shift in the presence of LY294002 (Fig. 3A).

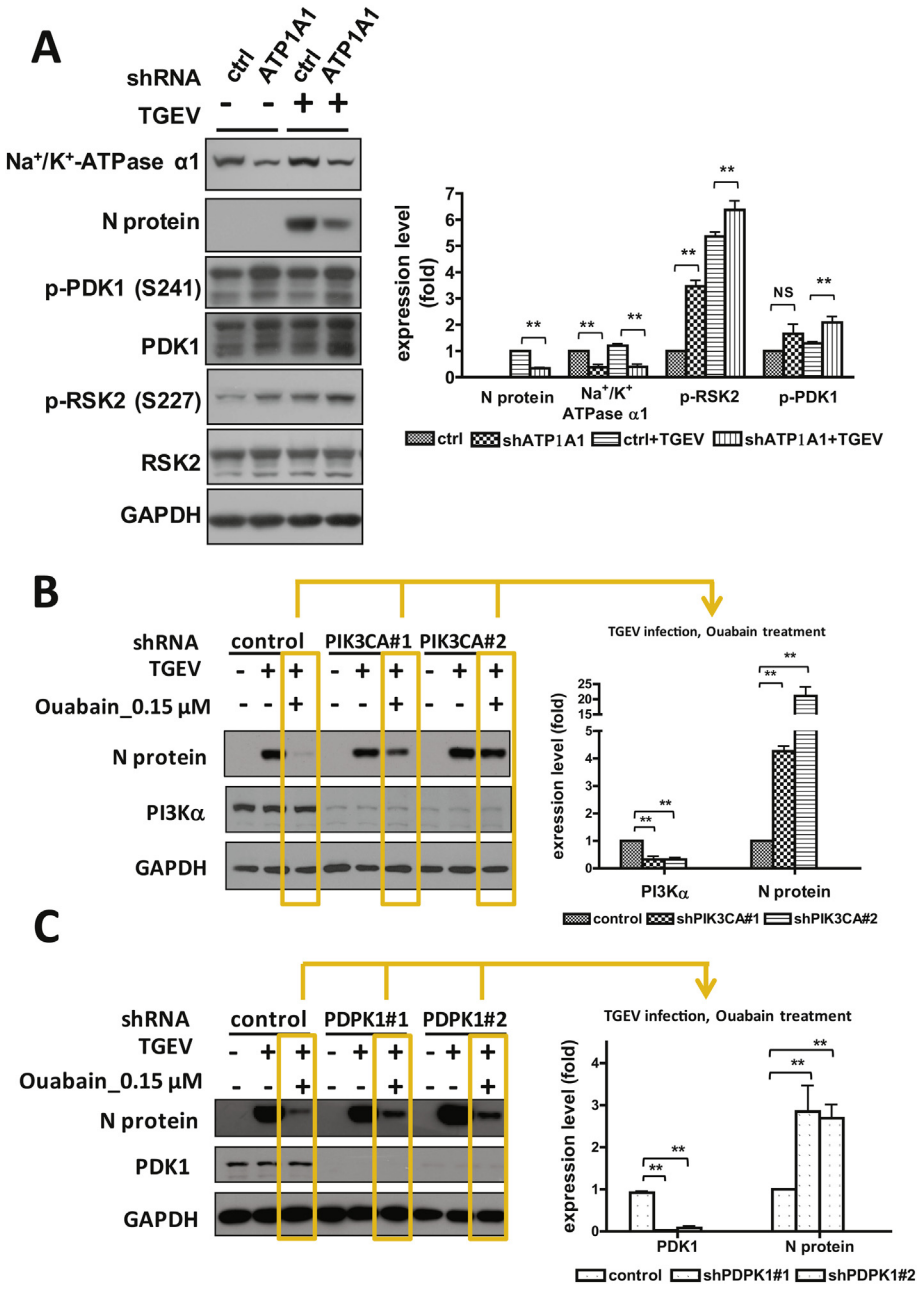

Fig. 5. The effects of knockdown expression of Na^+/K^+-ATPase α1, PI3K, or PDK1 on the TGEV activity. A. Knockdown of Na^+/K^+-ATPase α1 expression activated PI3K_PDK1_RSK2 axis pathway and suppressed TGEV activity. B & C. Knockdown of PI3K (B) or PDK1 expression (C) reversed the ouabain-inhibited TGEV activity/TGEV N protein expression. The validated knocked down cells were seeded onto a 6 well-plate, 1.8×10^6 cells/well, and cultured for 24 h prior to harvesting for western analysis with the antibodies indicated. NS: no significance; **, $P < .01$. Na^+/K^+-ATPase α1, p-PDK1, PI3Kα and N protein were normalized with GAPDH. p-RSK2 was normalized with regular RSK2. Results shown are represented results or averages ± SD from three independent experiments. The gene names for Na^+/K^+-ATPase α1, PDK1 and PI3Kα respectively are ATP1A1, PDPK1 and PIK3CA.

TGEV infection induced Akt phosphorylation, and ouabain treatment further augmented this Akt phosphorylation. The PI3K inhibitor LY294002 eliminated both TGEV induced and ouabain enhanced Akt phosphorylation (Fig. 3B). Ouabain has been reported to bind to Na^+/K^+-ATPase and resulted in recruitment for Na^+/K^+-ATPase associated signalsome, which in turn triggered signaling for the pharmacological effects of ouabain (Liu et al., 2007; Nguyen et al., 2011). This was supported by the observation that treatment with LY294002 inhibited the ouabain associated PI3K activation, as demonstrated by abolishing Akt phosphorylation; and rescued the TGEV N protein expression level – an indication of TGEV proliferation (Fig. 3B & C).

3.3. PDK1 activation mediated by ouabain enhanced PI3K activation was associated with Na^+/K^+-ATPase and contributed to anti-TGEV activity

A pharmacological inhibition strategy was used to examine the involvement of Akt, mTOR, and PDK1 (the downstream signaling cascades of PI3K) in the anti-TGEV activity of ouabain (Fig. 4A-B-C). Two doses of ouabain, 200 nM and 150 nM, close to its IC_{50} value (143 ± 13 nM) determined by IFA (Fig. 3A), were then used for the following studies (Figs. 4 and 5). The Akt inhibitor triciribine was able to inhibit Akt phosphorylation, but failed to rescue the diminished N protein expression by ouabain, as had been accomplished with the PI3K inhibitor LY294002 (Fig. 4A). Similarly, the mTOR inhibitor rapamycin was able to diminish the p70S6K phosphorylation, but failed to reverse the inhibited N protein expression by ouabain (Fig. 4B). Only the PDK1 inhibitor BX795 was able to reverse the ouabain-inhibited TGEV N protein expression. While ouabain treatment increased RSK2 phosphorylation (Fig. 4C), RSK1 phosphorylation was not significantly affected (data not shown). Treatment with BX795 inhibited the phosphorylation of PDK1 downstream effector RSK2 (Hao et al., 2016; No et al., 2015; Sun et al., 2017; Utepbergenov et al., 2016)(Fig. 4C).

Furthermore, in Na^+/K^+-ATPase α1 depleted ST cells infected by TGEV, TGEV N protein expression was significantly suppressed compared to those in control shRNA harboring ST cells (Fig. 5A) (Yang et al., 2017a), wherein PDK1 and RSK2 phosphorylation/activity were

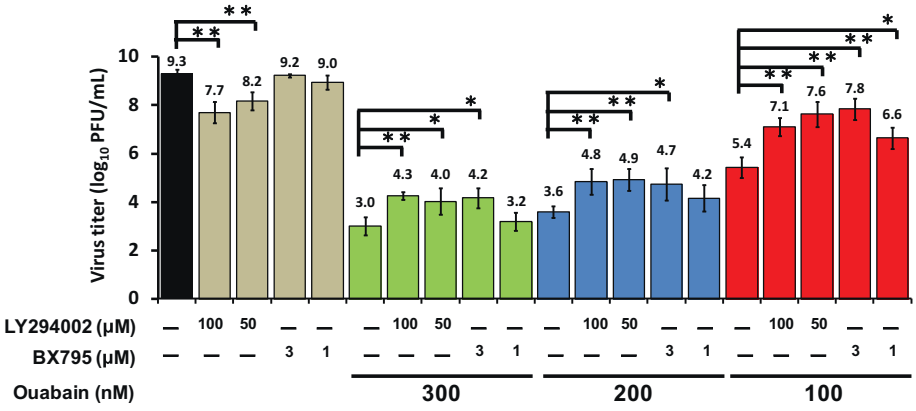

Fig. 6. Ouabain eliminated TGEV titers via augmenting a Na^+/K^+-ATPase dependent PI3K_PDK1 axis. Combined treatment of either LY294002 or BX795 with ouabain significantly rescued the TGEV replication/titers inhibited by ouabain. ST cells were pretreated with the indicated compounds for 1 h, and then infected with TGEV at a multiplicity of infection (MOI) of 0.01. The resultant cultured medium was harvested at 22 h.p.i. and subjected to determining virus titers by an end-point assay as described in Materials and Methods. *, $P < .05$; **, $P < .01$. Results shown are averages ± SD from three independent experiments.

significantly increased (Fig. 5A). Moreover, in PI3K or PDK1 depleted ST cells infected by TGEV, TGEV N protein expressions were in comparable amounts compared to those in control shRNA harboring ST cells (Fig. 5B & C). However, when these cells were treated with ouabain, the N protein was significantly suppressed in control shRNA harboring ST cells while depletion of PI3K or PDK1 was able to significantly reverse the ouabain-inhibited TGEV N protein expression (Fig. 5B & C).

Therefore, we concluded that ouabain targeted Na^+/K^+-ATPase and led to an enhanced PI3K_PDK1 axis signaling, which in turn imparted anti-TGEV activity.

3.4. Ouabain eliminated TGEV titers via an augmenting Na^+/K^+ATPase dependent PI3K_PDK1 axis

Ouabain potently eliminated TGEV titers in a dose-dependent manner (Fig. 1B); and both LY294002 (a PI3K inhibitor) and BX795 (a PDK1 inhibitor) blocked PI3K_PDK1_RSK2 signaling, antagonizing this effect (Figs. 3 and 4C). We further tested whether these effects resulted in diminishing virus titers. We found that LY294002 or BX795 significantly rescued the TGEV replication/titers inhibited by ouabain (Fig. 6). Thus, ouabain reduced TGEV viral replication/titers, at least in part, via enhancing an activated PI3K_PDK1 signaling cascade.

4. Discussion and conclusion

Cardenolides elevate the concentration of calcium in the cytoplasm, causing muscle contraction, and are thus used to treat cardiac dysfunction (Diederich et al., 2017). Recently, their use as anti-cancer drugs has been investigated (Baker Bechmann et al., 2016; Diederich et al., 2017). The underlying mechanisms of both processes, however, remain to be unraveled. Previously, we reported that cardenolides exert potent anti-viral activity in TGEV infected ST cells (Yang et al., 2017a). Herein, we disclose the results of our further investigations into the underlying mechanisms of this activity, and our discovery that the enhanced activation of PI3K_PDK1 axis in TGEV infected ST cells contributes to the anti-TGEV activity of ouabain.

Herein, cells were separately infected at MOIs of 7 (to screen compounds and dissect signaling pathways using western analyses, IFA etc.) and of 0.01 (to more accurately ascertain anti-viral potency). We first screened pharmacological inhibitors, in search of those which counteracted the anti-TGEV activity of ouabain. The PI3K inhibitor LY294002 was able to significantly counteract the anti-TGEV activity of ouabain (Table 2).

Recently, Na^+/K^+-ATPase α1 subunit mediated Src signaling was reported to inhibit another coronavirus, murine hepatitis virus, in HeLa cells transfected with a plasmid containing a human-derived but not murine-derived Na^+/K^+-ATPase α1 subunit (Burkard et al., 2015). We also reported that cardenolides do not exert anti- murine hepatitis virus activity in murine astrocytoma DBT cells (Yang et al., 2017a). However, no significant counteraction was found among the three Src inhibitors SU6656, PP2, and KX2–391 utilized herein for screening (Table 2) at the effective concentrations for signaling (data not shown). Thus, the role of Src signaling in anti-coronaviruses varies and depends on the nature of the Na^+/K^+-ATPase isoform and the exact cell type (Burkard et al., 2015; Yang et al., 2017a).

Additionally, although Src associated PI3K-Akt and PI3K-mTOR signaling cascades were reported to be responsible for the biological effects of the cardenolides in cardiac (Liu et al., 2007; Zhang et al., 2008) and cancer cells (Tian et al., 2009) respectively, ouabain also activates the Na^+/K^+-ATPase associated PI3K1A signaling, which is Src independent (Wu et al., 2013). Therefore, we further examined the downstream effectors of PI3K, Akt, mTOR, and PDK1, and found that only the PDK1 inhibitor BX795 was able to reverse the anti-TGEV activity of ouabain (Fig. 4). When Na^+/K^+-ATPase, not PI3K or PDK1, was knocked down in ST cells, a significant amount of N protein expression was suppressed, reflecting a decrease in virus infectivity. However, when PI3K or PDK1 was knocked down in ST cells, these cells became more resistant to ouabain treatment than control shRNA harboring ST cells, reflecting a reverse in virus infectivity (Fig. 5). Finally, combination treatments of either LY294002 or BX795 with ouabain successfully reversed the activity of the ouabain, and increased TGEV titers (Fig. 6).

Cardenolides have been used to treat hypotension and arrhythmia and the blood concentrations attained in patients are very low (Hauptman et al., 2013). Future development of the cardenolides for the treatment of coronavirus infection should be mindful of the in vitro observations reported herein, which should inform therapeutic dosage requirements.

In conclusion, the mechanism of action of the anti-TGEV activity of ouabain has been elucidated, and found to be mediated by the Na^+/K^+-ATPase-dependent PI3K_PDK1 axis, a novel cardenolide pharmacological signaling cascade. These fundamental mechanistic insights are expected to contribute to future applications of anti-viral cardenolides.

Conflict of interest

The authors declare no conflict of interest.

Acknowledgments

This work was funded by the Intramural funding from National Health Research Institutes, Taiwan, R.O.C. and the Ministry of Science and Technology, Taiwan, R.O.C. (Grants of: MOST 106-2320-B-400 -009 -MY3 and MOST 106-2811-B-400-025). We also would like to acknowledge the assistance from National RNAi Core Facility, Academia Sinica, Taiwan.

References

Agrawal, A.A., Petschenka, G., Bingham, R.A., Weber, M.G., Rasmann, S., 2012. Toxic cardenolides: chemical ecology and coevolution of specialized plant-herbivore interactions. New Phytol. 194, 28–45.

Baker Bechmann, M., Rotoli, D., Morales, M., Maeso Mdel, C., Garcia Mdel, P., Avila, J., Mobasheri, A., Martin-Vasallo, P., 2016. Na,K-ATPase isozymes in colorectal cancer and liver metastases. Front. Physiol. 7, 9.

Burkard, C., Verheije, M.H., Haagmans, B.L., van Kuppeveld, F.J., Rottier, P.J., Bosch, B.J., de Haan, C.A., 2015. ATP1A1-mediated Src signaling inhibits coronavirus entry into host cells. J. Virol. 89, 4434–4448.

Delmas, B., Gelfi, J., L'Haridon, R., Vogel, L.K., Sjostrom, H., Noren, O., Laude, H., 1992. Aminopeptidase N is a major receptor for the entero-pathogenic coronavirus TGEV. Nature 357, 417–420.

Diederich, M., Muller, F., Cerella, C., 2017. Cardiac glycosides: from molecular targets to immunogenic cell death. Biochem. Pharmacol. 125, 1–11.

Habeck, M., Tokhtaeva, E., Nadav, Y., Zeev, E.B., Ferris, S.P., Kaufman, R.J., Bab-Dinitz, E., Kaplan, J.H., Dada, L.A., Farfel, Z., Tal, D.M., Katz, A., Sachs, G., Vagin, O., Karlish, S.J.D., 2016. Selective assembly of Na,K-ATPase α2β2 heterodimers in the heart: distinct functional properties and isoform-selective inhibitors. J. Biol. Chem. 291, 23159–23174.

Hao, Y., Samuels, Y., Li, Q., Krokowski, D., Guan, B.J., Wang, C., Jin, Z., Dong, B., Cao, B., Feng, X., Xiang, M., Xu, C., Fink, S., Meropol, N.J., Xu, Y., Conlon, R.A., Markowitz, S., Kinzler, K.W., Velculescu, V.E., Brunengraber, H., Willis, J.E., Laframboise, T., Hatzoglou, M., Zhang, G.F., Vogelstein, B., Wang, Z., 2016. Oncogenic PIK3CA mutations reprogram glutamine metabolism in colorectal cancer. Nat. Commun. 7, 11971.

Hauptman, P.J., McCann, P., Romero, J.M., Mayo, M., 2013. Reference laboratory values for digoxin following publication of Digitalis Investigation Group (DIG) trial data. JAMA Intern. Med. 173, 1552–1554.

Katz, A., Tal, D.M., Heller, D., Habeck, M., Ben Zeev, E., Rabah, B., Bar Kana, Y., Marcovich, A.L., Karlish, S.J., 2015. Digoxin derivatives with selectivity for the alpha2beta3 isoform of Na,K-ATPase potently reduce intraocular pressure. Proc. Natl. Acad. Sci. U. S. A. 112, 13723–13728.

Liu, L., Zhao, X., Pierre, S.V., Askari, A., 2007. Association of PI3K-Akt signaling pathway with digitalis-induced hypertrophy of cardiac myocytes. Am. J. Phys. Cell Phys. 293, C1489–C1497.

Nagai, Y., Maeno, K., Iinuma, M., Yoshida, T., Matsumoto, T., 1972. Inhibition of virus growth by ouabain: effect of ouabain on the growth of HVJ in chick embryo cells. J. Virol. 9, 234–243.

Newman, R.A., Yang, P., Pawlus, A.D., Block, K.I., 2008. Cardiac glycosides as novel cancer therapeutic agents. Mol. Interv. 8, 36–49.

Nguyen, A.N., Jansson, K., Sanchez, G., Sharma, M., Reif, G.A., Wallace, D.P., Blanco, G., 2011. Ouabain activates the Na-K-ATPase signalosome to induce autosomal dominant polycystic kidney disease cell proliferation. Am. J. Physiol. Ren. Physiol. 301, F897–F906.

No, Y.R., He, P., Yoo, B.K., Yun, C.C., 2015. Regulation of NHE3 by lysophosphatidic acid is mediated by phosphorylation of NHE3 by RSK2. Am. J. Physiol. Cell Physiol. 309, C14–C21.

Oh, J.S., Song, D.S., Park, B.K., 2003. Identification of a putative cellular receptor 150 kDa polypeptide for porcine epidemic diarrhea virus in porcine enterocytes. J. Vet. Sci. 4, 269–275.

Platz, E.A., Yegnasubramanian, S., Liu, J.O., Chong, C.R., Shim, J.S., Kenfield, S.A., Stampfer, M.J., Willett, W.C., Giovannucci, E., Nelson, W.G., 2011. A novel two-stage, transdisciplinary study identifies digoxin as a possible drug for prostate cancer treatment. Cancer Discov. 1, 68–77.

Prassas, I., Diamandis, E.P., 2008. Novel therapeutic applications of cardiac glycosides. Nat. Rev. Drug Discov. 7, 926–935.

Su, C.T., Hsu, J.T., Hsieh, H.P., Lin, P.H., Chen, T.C., Kao, C.L., Lee, C.N., Chang, S.Y., 2008. Anti-HSV activity of digitoxin and its possible mechanisms. Antivir. Res. 79, 62–70.

Sun, C., Sun, Y., Jiang, D., Bao, G., Zhu, X., Xu, D., Wang, Y., Cui, Z., 2017. PDK1 promotes the inflammatory progress of fibroblast-like synoviocytes by phosphorylating RSK2. Cell. Immunol. 315, 27–33.

Tian, J., Li, X., Liang, M., Liu, L., Xie, J.X., Ye, Q., Kometiani, P., Tillekeratne, M., Jin, R., Xie, Z., 2009. Changes in sodium pump expression dictate the effects of ouabain on cell growth. J. Biol. Chem. 284, 14921–14929.

Tomita, Y., Kuwata, T., 1978. Suppression of murine leukaemia virus production by ouabain and interferon in mouse cells. J. Gen. Virol. 38, 223–230.

Utepbergenov, D., Hennig, P.M., Derewenda, U., Artamonov, M.V., Somlyo, A.V., Derewenda, Z.S., 2016. Bacterial expression, purification and in vitro phosphorylation of full-length ribosomal S6 kinase 2 (RSK2). PLoS One 11, e0164343.

Weingartl, H.M., Derbyshire, J.B., 1995. Cellular receptors for transmissible gastroenteritis virus on porcine enterocytes. Adv. Exp. Med. Biol. 380, 325–329.

Weiss, S.R., Navas-Martin, S., 2005. Coronavirus pathogenesis and the emerging pathogen severe acute respiratory syndrome coronavirus. Microbiol. Mol. Biol. Rev. 69, 635–664.

Wu, J., Akkuratov, E.E., Bai, Y., Gaskill, C.M., Askari, A., Liu, L., 2013. Cell signaling associated with Na(+)/K(+)-ATPase: activation of phosphatidylinositide 3-kinase IA/Akt by ouabain is independent of Src. Biochemistry 52, 9059–9067.

Yang, C.W., Yang, Y.N., Liang, P.H., Chen, C.M., Chen, W.L., Chang, H.Y., Chao, Y.S., Lee, S.J., 2007. Novel small-molecule inhibitors of transmissible gastroenteritis virus. Antimicrob. Agents Chemother. 51, 3924–3931.

Yang, C.W., Chang, H.Y., Hsu, H.Y., Lee, Y.Z., Chang, H.S., Chen, I.S., Lee, S.J., 2017a. Identification of anti-viral activity of the cardenolides, Na+/K+-ATPase inhibitors, against porcine transmissible gastroenteritis virus. Toxicol. Appl. Pharmacol. 332, 129–137.

Yang, C.W., Lee, Y.Z., Hsu, H.Y., Shih, C., Chao, Y.S., Chang, H.Y., Lee, S.J., 2017b. Targeting Coronaviral replication and cellular JAK2 mediated dominant NF-kappaB activation for comprehensive and ultimate inhibition of coronaviral activity. Sci. Rep. 7, 4105.

Zhang, L., Zhang, Z., Guo, H., Wang, Y., 2008. Na+/K+-ATPase-mediated signal transduction and Na+/K+-ATPase regulation. Fundam. Clin. Pharmacol. 22, 615–621.